Journal Pre-proofs

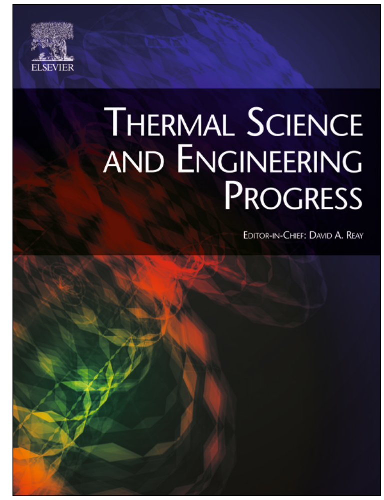

Numerical investigation of indoor thermal comfort and air quality for a multi-purpose hall with various shading and glazing ratios

Reza Amini, Amirhosein Ghaffarianhoseini, Ali Ghaffarianhoseini, Umberto Berardi

PII: S2451-9049(20)30332-2
DOI: https://doi.org/10.1016/j.tsep.2020.100812
Reference: TSEP 100812

To appear in: *Thermal Science and Engineering Progress*

Received Date: 26 July 2020
Revised Date: 10 December 2020
Accepted Date: 10 December 2020

Please cite this article as: R. Amini, A. Ghaffarianhoseini, A. Ghaffarianhoseini, U. Berardi, Numerical investigation of indoor thermal comfort and air quality for a multi-purpose hall with various shading and glazing ratios, *Thermal Science and Engineering Progress* (2020), doi: https://doi.org/10.1016/j.tsep.2020.100812

Numerical investigation of indoor thermal comfort and air quality for a multi-purpose hall with various shading and glazing ratios

Reza Amini, ramini@mr-cfd.com, MR CFD LLC, Tbilisi, Georgia

Amirhosein Ghaffarianhoseini, Department of Built Environment Engineering, Auckland University of Technology, New Zealand

Ali Ghaffarianhoseini, Department of Built Environment Engineering, Auckland University of Technology, New Zealand

Umberto Berardi, Faculty of Engineering and Architectural Science, Ryerson University, Canada

Abstract

This research assesses the effect of outdoor parameters, including solar radiation and shading and glazing configurations, on indoor thermal comfort and air quality in multi-purpose halls in Auckland, New Zealand. The Design of experiment (DOE) method by using CFD simulation has been used for this study. Input parameters are windows length, overhang angle, and overhang length, while output parameters are occupant zone average temperature and mass fraction. The temperature sensitivity to the glazing parameter changes with time, and its maximum occurs at 11:00 and is 95%, while for shading ones happen at 9:00 and is 50%. The peak of CO2 mass fraction sensitivity to glazing and shading parameters coincides at 9:00 and is 90% and 80, respectively. The variation rate of temperature and CO2 mass fraction VS. Glazing parameter (W.L) is approximately positive on the summer day. However, it has nonlinear and complex behavior, while shading one has a sinusoidal behavior. On the other side, On the winter day, the temperature variation rate is almost linear regarding this factor. The result shows that appropriate shading and glazing situation for each time is different, and for reaching the best comfort, dynamic shading and glazing should be designed. Comfort criteria sensitivity within the school is highly dependent on glazing parameters compared with shading configurations. The temperature can be controlled up to 3 and 1.6 degrees in the summer winter day, respectively. Finally, it can be concluded that glazing tools can compensate for a significant amount of required heating in the winter days, and shading devices and opening windows can control the air quality in the school buildings with neglectable overheating.

Keywords: Thermal comfort, indoor air quality, response surface, solar energy, computational fluid dynamics.

Nomenclature

C_p	Specific heat (J. Kg^{-1}. K^{-1})	$\vec{s}$	Direction vector
D	Diffusion coefficient of chemical species ($m^2.s^{-1}$)	$\overrightarrow{r,}$	Position vector
IIAQ	Index of Indoor air quality	t	Time (s)
g	Gravity acceleration ($m.s^{-2}$)	T	Temperature (K)
k	Turbulent kinetic energy ($m^2.s^{-2}$)	U	Velocity modulus ($m.s^{-1}$)
L	Characteristic length (m)	u_i	Velocity components ($m.s^{-1}$)
n	Normal direction	x_i	Coordinates (m)
p	Fluid pressure (Pa)	***Greek symbols***	
$\overrightarrow{r,}$	Direction (m)	α	Thermal diffusivity ($m^2.s^{-1}$)
a_λ	Spectral absorption coefficient	ε	Turbulent energy dissipation ($m^2.s^{-3}$)
n	Refractive index	λ	Thermal conductivity ($W.m^{-1}K^{-1}$)
$(a_\lambda + \sigma_\lambda)$	Optical thickness	μ	Dynamic viscosity ($kg.m^{-1}s^{-1}$)
$I_{b\lambda}$	Black body intensity	ρ	Density of the mixture ($kg.m^{-3}$)
J	Diffusion flux	φ	Concentration
E_{ij}	dissipation tensor	$C_1\varepsilon$, $C_2\varepsilon$	constants of transport equations
I_λ	irradiation intensity	Ω'	Spatial angle

1. Introduction

Due to the rising level of pollution and its relationship with health problems, more attention has been given to indoor air quality in recent years. New building designs pay much more attention to insulation and save energy, which significantly impacts indoor air quality [1, 2]. For this reason, higher ventilation rates are recommended to improve indoor air quality, which should perform well in removing pollutants from indoor air [3-5]. On the other hand, thermal comfort has a particular importance, as it interacts with well-being, energy consumption, and productivity, particularly in schools [6]. A proper school building design results in a standard teaching space quality in terms of temperature and pollution, significantly influencing teachers' and students' health and educational achievement. The building design has a crucial impact on energy consumption and other natural resources, while the building energy consumption ratio to total energy demand is about 35.3% [7]. Some previous studies have revealed that the thermal comfort and IAQ of the schools are significantly below the standard levels. As a case in point, Pereira *et al.* conducted a survey-based analysis from students of a school in Portugal. Results showed that thermal comfort and IAQ were lower than standard level [8], and Al-Hubail *et al.* concluded that at 54% and 24% of schools, PM10, and CO_2 concentration, respectively, are higher than the allowed standards in the State of Kuwait with the desert climate [9]. High or low temperature, relative humidity, and velocity lead to thermal discomfort [10] that both issues have been lead to a decrease in children's performance during education [11-13]. The thermal distribution and IAQ of schools have been investigated in several recent studies. Asere *et al.* investigated the indoor air quality in some educational buildings and concluded that CO_2 levels were reported as 2707 ppm, and it can be concluded that the rate of air change was very low and should be increased. [14]. For the standard level of IAQ, ASHRAE recommends CO_2 levels not exceeding 700 ppm above outdoor levels [15]. In order to evaluate indoor thermal comfort, Two standards, ASHRAE 55[16] and ISO 7730[17] in parallel, is developed. Both of them use two indices by the name of predicted mean vote (PMV) and predicted percentage of dissatisfied (PPD) that depends on six factors, including metabolic rate, Clothing insulation, Radiant temperature, Air temperature, speed, and humidity. Three of them (velocity, humidity, and temperature of the air) can be extracted from CFD simulation. In this research, temperature and velocity that is entirely coupled together is investigated and humidity variation investigation is neglected. Since using passive method for heating and cooling can con not satisfied all of requirement energy for this building and vast majority amount of this energy should be provided by active HVAC system. Thermal comfort indices that represent the local thermal situation cannot be used and in this research average output parameter is investigated. One of future studies for this project can be adding a mechanical ventilation n system and thermal comfort analysis based on PMV and PPD indices.

To evaluate indoor thermal comfort, Two standards, ASHRAE 55[16] and ISO 7730[17] in parallel, is developed. Both of them use two indices by the name of predicted mean vote (PMV) and predicted percentage of dissatisfied (PPD) that depends on six factors, including metabolic rate, Clothing insulation, Radiant temperature, Air temperature, speed, and humidity. Three of them (velocity, humidity, and temperature of the air) can be extracted from CFD simulation. In this research, temperature and velocity that are entirely coupled together are investigated and humidity variation investigation is neglected. Since using a passive method for heating and cooling can con not satisfied all of the required energy for this building and the vast majority amount of this energy should be provided by an active HVAC system. Thermal comfort indices that represent the local thermal situation cannot be used and in this research average output parameter is investigated. One of the future studies for this project can be adding a mechanical ventilation n system and thermal comfort analysis based on PMV and PPD indices

Griffiths *et al.* concluded that the IAQ of the classroom is at an acceptable level when the CO_2 concentration does not exceed 1000 ppm [18]. The primary sources of this emission generation in the classroom are student and teachers respiratory systems where CO_2 more than 1000 ppm in a classroom results in yawn and dizziness for students [19]. Vilcekova *et al.* experimentally recorded the average indoor air temperature, relative humidity, and CO_2 concentration for a school in the summer and winter seasons. They proposed that to increase indoor air quality, thermal comfort, and optimization measures are needed [20]. Stabile *et al.* studied the effects of different natural ventilation situations on the concentration of CO_2 and the number of particles directly affecting

Italian classrooms' indoor air quality. they concluded that manual airing outdoors is not appropriate for reducing all pollutant species [21]. Razali *et al.* investigated schools in Malaysia and found that the outdoor air quality has the minimum impact of classroom IAQ except for schools near busy roads [22]. Dynamic control of ventilation strategy means that using an automated, regulated ventilation rate to provide good IAQ reduces energy cost and makes a delay in starting mechanical ventilation [23]. Athienitis *et al.* concluded that the building's energy requirement would be intensively decreased using a controllable shading device. [24]. Designing proper ventilation for an educational building by considering the least energy consumption and passive methods is complicated. During winter, the windows are closed to decrease heat loss, while the lack of fresh air causes low IAQ. On the other side, Increasing the window-to-wall ratio (WWR) to achieve high IAQ in summer may increase winter heat loss. For designing passive ventilation, it is essential to protect windows from solar radiation during summer days by various methods like shading tools [25]. The main reason for the application of shading device is to control the direct solar radiation [26]. Shading configuration mainly depends on building shape and orientation [27]. Park *et al*. proved that using overhang, regardless of wind velocity, leads to an increase in air change per hour (ACH) [28]. Yao showed that by using vertical moving shading, building energy demand will reduce by 30.87%, and thermal comfort improves by 21% in China [29]. By concerning the overheating phenomena in glazed buildings, Simmler *et al.* carried out various experiments and numerical simulations [30]. Poirazis *et al.* investigated a sensitivity analysis of a single skin glazed office building. The main parameter that they have investigated was the window to wall ratio, the building's orientation, and the configuration of the façade. They concluded that careful design based on thermal simulation should be carried out to decrease energy consumption and promote thermal comfort, especially for the highly glazed building [31]. Various software is available to calculate thermal comfort during the days [25]. However, it is concluded that the studied methods to calculate the average temperature conditions neglect the significance of calculating local ventilation conditions. Depends on the building locations, climate conditions and etc. various type of shading device can be used. In this article adjustable horizontal shading device instead of fixed one is used to avoid leakage of solar radiation during the morning or afternoon. Currently, CFD simulation is predominantly popular for evaluating the natural ventilation in buildings as it provides highly accurate information compared to Zonal Approach methods. Therefore, CFD models have been applied in many studies to assess and optimize the natural ventilation of buildings [32]. Table 1 indicates a summary of recent natural ventilation and thermal comfort studies in buildings based on CFD simulations. It also indicates the object of analysis, significant findings and observations derived from each study. Moreover, a new optimization method, including a Design of Experiments (DOE) with genetic aggregation response surface methodology (RSM) can be employed to achieve the optimal parameters of the simulated model, in terms of indoor thermal comfort and air quality. Abdeen *et al.* used this method to improve indoor airflow and obtain the solar chimney's optimal parameters connected to a building [33]. In the northern part of New Zealand, the Auckland region experiences a subtropical climate that is warm and humid in summer and mildly cold in winter [34]. The maximum temperature in summer is below the maximum allowable world organization health. Hence, there is no pressing need for cooling in the summer, however, considering shading and glazing configuration at different times of the day, different building zones will be overheated, and it is necessary to use pedestal ceiling fans to overcome this issue. However, winter's minimum temperature is lower than the permissible temperature to have standard thermal comfort [35]. Although this difference is not significant, and by consuming little energy for heating, it can be compensated.

Many simulations have been done to investigate thermal comfort and indoor air quality in buildings in various locations. Most of them have been done with methods that have examined the building's overall thermal behavior and have not addressed the local temperature and airflow behavior. Especially the effect of solar radiation at various times of the day can be modeled in detail. The CFD simulation can evaluate the quality of local ventilation in every building zone. Local improvement of the building's comfort will be more comfortable and accurate, leading to optimizing energy consumption. As mentioned in Table 1, several CFD simulation studies have been done in various office buildings, and they have evaluated thermal comfort situations, with no focus on indoor air quality.

Table 1: A summary of recent natural ventilation and thermal comfort studies in buildings based on CFD simulations

Main Focus	Major Findings/Observations	Ref.
The effect of natural airflow of schools on thermal comfort	The classrooms' airflow rate at upper levels is higher than that in the lower levels, and this trend is similar for the three dominant winds from the north, northeast, and south.	[36]
Impact of louvers on cross-ventilation in an isolated building	Opening situated in the upper part of the building shell provide the highest volume flow rate. Opening situated in the center provides the highest air exchange efficiency.	[37]
Evaluation of natural cross ventilation of a building with CFD	Wind velocity on the building roof and the apartment's airflow rate can be accessed via CFD with acceptable accuracy.	[38]
Evaluation of indoor natural ventilation according to the window parameters	A 2.5% decrease in air temperature and a 6-fold increase in air velocity can be achieved by optimizing window parameters.	[39]
A method for assessing natural indoor ventilation in hot climates	Calculate the indoor air velocity in hot climates causes the Heat Balance Index (HBI) method to provide more accurate results.	[40]
Impact of ventilated office buildings on visual and thermal comfort	The connections between buildings and street layout are well illustrated by parametric analysis. A similar building configuration for each climate was concluded for the best ventilation purposes. The ratio of 0.3 windows to the wall is the optimal value for reducing the solar gains and removing the external overhangs.	[41]

The efficiency of natural greenhouse ventilation	64% of maximum heat can be removed with the closed windward roof vent and open wall vent. Wind direction as the key element to improve the system of vent control has been suggested.	[42]
Air movement in low-rise buildings with non-rectangular floor-plan	Natural airflow has the potential to reduce the building's cooling requirement by 65%.	[43]
Cross ventilation in the presence of wind catcher ventilation. **Evaluation of building was based on three critical factors, including induced airflow rate, air exchange performance, and air age**.	Outlet opening should not be closed to the wind catcher because it leads to a significant decrease in the IAQ, and on the other hand, the best suggestion is to use a one-sided wind catcher and windows simultaneously.	[44]
Natural ventilation in underground constructions	The access tunnel is the crucial element in the ventilation of underground construction, where the ground temperature plays an essential role in regulating natural ventilation.	[45]
Comparison of volume flow rate and the volume-averaged local mean age of air for evaluating ventilation performance	The volume-averaged Local mean age of the airfield was a more accurate representation of the building's local ventilation performance than the velocity vector field.	[46]

Table 1 Continuation

Main Focus	Major Findings/Observations	Ref.
Finding the Impact of a void connected to the multi-story housing on natural ventilation.	A 50.88 % increase in air velocity can be achieved in the living units by increasing the void dimensions to 50% of the living spaces.	[47]
Impact of a windward window and various wind exchangers on natural ventilation	The flow distribution in the living room is the critical factor for selecting the wind exchanger configuration and the volume flow rate.	[48]
Assessing of natural airflow of High-rise building with balcony	The speed of cross ventilation was reduced by adding a balcony. The balcony has a positive effect on single-sided ventilation and improves it.	[49]
Assessing the indoor air quality of a building concerning air pollution caused by traffic	Indoor air quality in naturally ventilated buildings is weaker than the external environment.	[50]
Evaluating CFD simulation by solving the RANS turbulence model for **air quality assessment caused by temperature stratification.**	RANS CFD simulation can predict temperature stratification	[51]

CFD simulation of two ventilation method simultaneously and predicting the **air quality and t**he t**hermal comfort**	Passive child beams can compensate for the temperature gradient caused by the displacement ventilation method	[52]
Study the **air quality and thermal comfort of a kitchen room** with different exhaust volumes	By increasing the air volume flow rate, satisfaction will be raised.	[53]
Thermal comfort and indoor air quality assessment in the presence of a smart windows ventilation (SWV) integrated system coupled with an active system.	Applying the SWV system conjugated with an active system has better thermal comfort and IAQ performance in winter than in the summer.	[54]
Predicting the pressure coefficient of a building in the presence of single shaded louvers.	The windward section's pressure coefficient is maximum compared, and another critical factor that they reached was the best performance of the horizontal louvers would occur when the angle of them is between 60° to 75°.	[55]

Also, the effect of using shading and glazing devices on these two essential qualities in educational buildings has not been studied so far. The coupled interaction of these two parameters has not been considered before, while these parameters' effects cannot be studied separately. It means that by changing the shading configuration, buildings' thermal comfort and air quality behavior are changed compared to the glazing parameter, and vice versa. The computational cost for all the experiments' simulation is about ten times more than using the DOE method. Therefore, this method is the best-suggested method for satisfying this goal. A few kinds of research using computational fluid dynamics has been done on air conditioning in school buildings for Auckland's geographical location. This study investigates shading and glazing configurations' capability to investigate the indoor thermal comfort and IAQ in a multi-purpose hall by evaluating the corresponding parameters' interactive impact. The central composite design of DOE methodology has been used to reduce the number of experiments and investigate the simultaneous effects of shading and glazing parameters. The genetic aggregation method has been used to obtain the response surface of the obtained results.

2. Methodology

2.1 Geometry

As shown in Figure 1, the simplified geometry of a multi-purpose hall with a central courtyard with twelve windows and overhangs has been used in this study. Geometry dimensions are 10×10×4 m with a 3×3×4 m central courtyard. The length, angle of the overhang, and window length will change at various design points. During summer, it was assumed that all windows are open, while during winter, the windows are closed (outdoor temperature is lower than standard), which requires an active ventilation method to increase IAQ in this season. Solar radiation angle during winter is lower than in summer, and since shading study in this season is not the aim of this research, the overhang during winter was not applied, and only thermal comfort was studied. Since this research's primary focus is on passive ventilation, the summer season's main active parameter is the overhangs and windows length and angle.

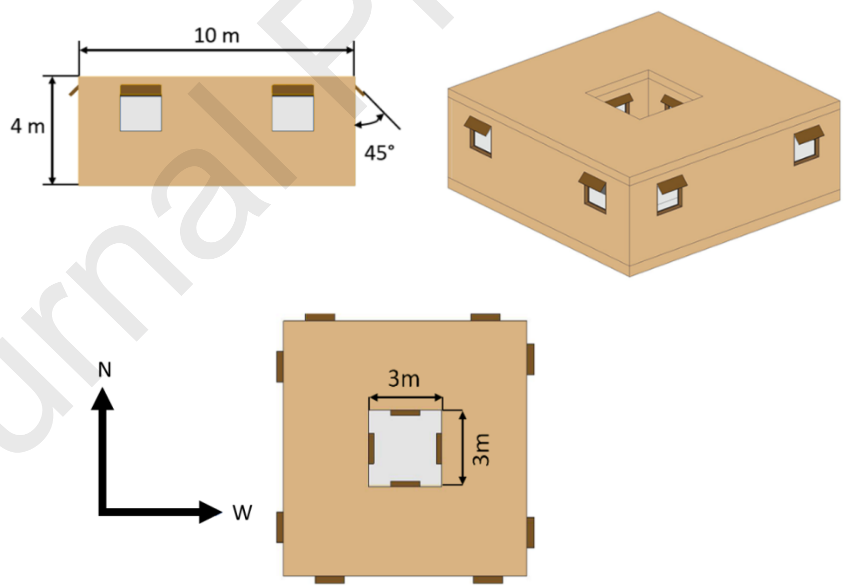

Figure 1. Schematic of the multi-purpose hall with windows, overhang, and courtyard

2.2 Computational fluid dynamics models

In the reviewed literature, different turbulence models have been employed to model turbulence effects. Among them, Rouaud *et al.* conducted a turbulence sensitivity analysis for all of the K-Epsilon sub-model. Their result showed that the RNG sub-model could simulate the fluid flow of air and determining turbulent intensity [56]. Chen *et al.* investigated the application of two K-Epsilon sub-models for a free and forced convection in a room with applying a jet stream; they found out that the RNG turbulence model has a better result [57].

In this research, a commercial Reynolds-Averaged Navier-Stokes (RANS) finite volume code (ANSYS FLUENT 2019 R3) was used to perform these simulations. Ideal gas density law is used for considering the buoyancy effect in the classrooms. The species transport model applying first Fick's law predicts the CO_2 generation and its diffusion, convection, and distribution in the building. Outdoor CO_2 mass fraction is 400 ppm[58], and the student's and teacher's respiratory system is supposed to be a primary indoor CO_2 source. The RNG K-ε model is used to solve turbulence effects, and the PISO method is employed for coupling the velocity and pressure equations. The energy equation is enabled to predict temperature distribution, and the DO radiation model is used to determine volumetric radiation calculation and consider the effect of air on absorbing and scattering radiation. This model can solve semi-transparent wall radiation in an appropriate angle discretization. This model's computational cost and memory requirement are relatively low. In this model, using a gray band, it is possible to solve the problem by the assumption of gray or non-gray radiation [59]. The solar ray-tracing model is used to determine the solar radiation and direction in each time and location, while in this method, the solar load is applied to the energy equation as a source term. There is a calculator that, by selecting the day, hours, and particular position on the ground, the sun location direction vector in the sky can be calculated [60]. Five and Four different hours during the day are selected for summer and winter days, respectively. It is evident that the solar radiation magnitude and direction entirely depend on the time of the day. Therefore, the optimized configuration at each time will be different.

The governing equation is used as the general form as follows:

Continuity equation:

$$\nabla.(\rho u) = 0 \tag{1}$$

Momentum equation

$$\mu\nabla^2 u + \frac{1}{3}\mu\nabla(\nabla.u) + \rho g = \nabla p \tag{2}$$

The equations of the K-ε turbulence model are as follows:

Turbulence kinetic energy equation:

$$\frac{\partial(\rho\varepsilon u_i)}{\partial x_i} = \frac{\partial}{\partial x_j}\left[\frac{\mu_t \partial k}{\sigma_k \partial x_j}\right] + 2\mu_t E_{ij} E_{ij} - \rho\varepsilon \tag{3}$$

Turbulence dispersion equation:

$$\frac{\partial(\rho\varepsilon u_i)}{\partial x_i} = \frac{\partial}{\partial x_j}\left[\frac{\mu_t \partial \varepsilon}{\sigma_\varepsilon \partial x_j}\right] + C_{1\varepsilon}\frac{\varepsilon}{k} 2\mu_t E_{ij} E_{ij} - C_{2\varepsilon}\rho\frac{\varepsilon^2}{k} \tag{4}$$

Energy equation:

$$\rho\left[u\frac{\partial E}{\partial x} + v\frac{\partial E}{\partial y} + w\frac{\partial E}{\partial z}\right] = \nabla.(k\nabla T) - \nabla.p\vec{v} + Q_v + Q_g \tag{5}$$

Fick's law of diffusion:

$$j = -D\frac{d\varphi}{dx} \tag{6}$$

Radiation equation:

$$\nabla.\left(I_\lambda(\overrightarrow{r,\vec{s}})\vec{s}\right) + (a_\lambda + \sigma_\lambda)I_\lambda(\overrightarrow{r,\vec{s}}) = a_\lambda n^2 I_{b\lambda} + \frac{\sigma_s}{4\Pi}\int_0^{4\Pi} I_\lambda(\overrightarrow{r,\vec{s}})\varphi(\vec{s}.\vec{s}')d\Omega' \quad (7)$$

2.3 Validation

M.L.pereira *et al.* studied the effect of several configurations of ventilation on thermal comfort, air velocity, and IAQ [61]. They used several lamps to model solar radiation. In the current study, solar radiation is the primary input parameter that affects thermal comfort. The result of their research is used to validate the numerical simulation. The configuration used as a base is ceiling supply and return to the near floor. The temperature distribution in the direction of building height has been compared with numerical simulation. Both effects of buoyancy flow and forced convection are considered the main ways of heat transfer in building, and the ideal gas law is used to predict the density of air in different temperature distribution. Also, since there is a zone with a high-temperature situation, the radiation effect should be considered. Because of the high relevance between temperature and velocity distribution, sensitivity analysis is done in various RANS turbulence models.

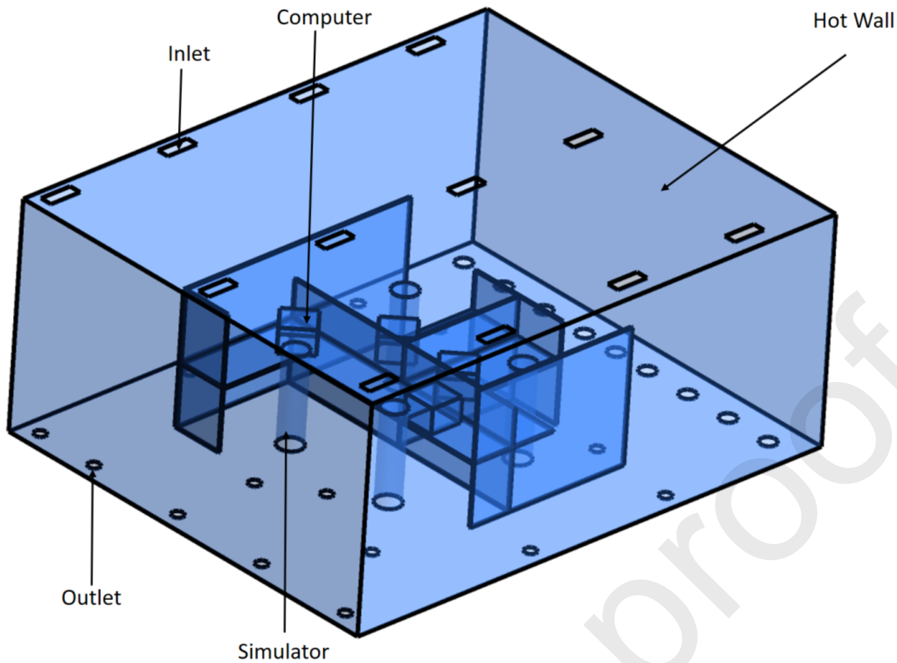

Figure 2. The geometry of the simulated room

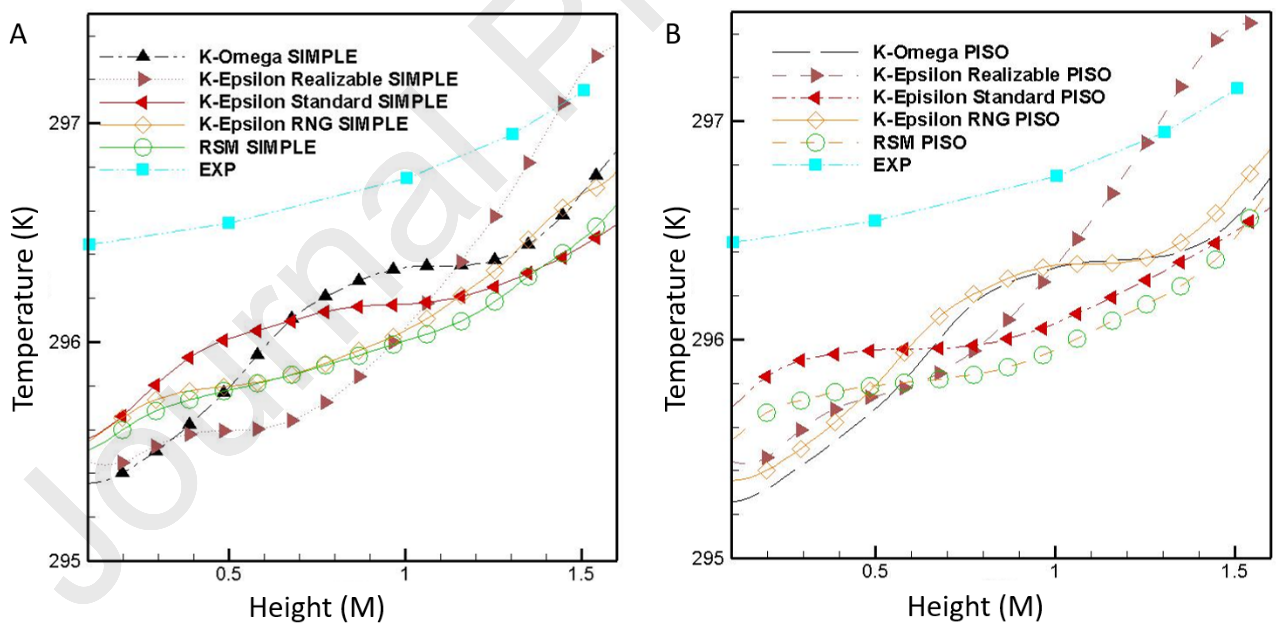

Figure 3. Temperature validation with turbulence sensitivity analysis, A: SIMPLE methods B: PISO method.

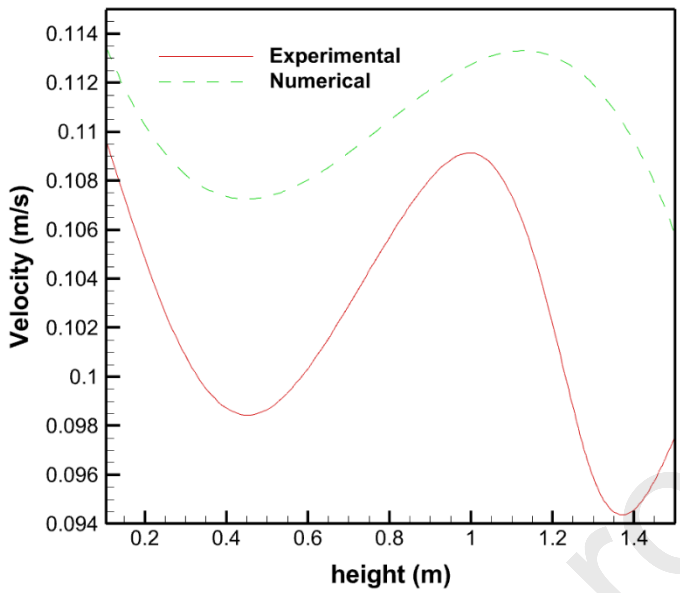

Figure 4. velocity validation with experimental data in the direction of height

The simulation room's geometry is shown in Figure 2 and, the turbulent sensitivity analysis results to find the best-fit equation for validating temperature are shown in Figure3. Both SIMPLE and PISO methods are used for the pressure coupling method and compared with experimental results. The second-order upwind discretization scheme is used to solve the density, momentum, turbulence, energy, and discrete ordinated equations. The results show that the maximum error occurs at the bottom and is below 4% in all turbulence models, which is entirely acceptable. So, for predicting the magnitude of temperature, all methods are acceptable. However, the temperature gradient comparison between numerical and experimental results should also be made since its accuracy in the direction of the building's height is crucial and must be lower than 3 K/1.8m (human height). It is shown that the Reynolds Stress Model (RSM) and K-ε RNG temperature gradient is closer to experimental results than the rest of the turbulence methods. There is a significant difference between RSM and experimental results in the mean height values. Hence, k-epsilon RNG is selected for the turbulence method. The temperature gradient belongs to the PISO method result is lower than the SIMPLE ones and is closer to that of experimental. In this section's conclusion, the assumption of using ideal gas for destiny rule, the k-ε RNG method for the turbulence model, PISO pressure coupling method, and DO radiation model can predict temperature distribution by considering solar radiation and wind speeds. Although in this research, the effect of wind speed on the indoor ventilation situation is neglected. Since in this work, the focus area is on the thermal comfort and IAQ, and the other hand, IAQ highly depends on the velocity field, Figure 4 shows the velocity validation with experimental data based on the previous method, and the result shows that these methods can predict velocity filed with acceptable accuracy, in a way that the minimum and the maximum error is 7 and 13 percent, respectively.

2.4 Boundary and zone condition

No-slip boundary condition with thermal convection condition is used for all of the walls. All wall participates in solar ray tracing. The solar radiation intensity and direction highly depend on the building's location and the time of the experiment. Five and flour different solar radiation, diffusion, and direction for five hours are applied for summer and winter. This magnitude can be seen in table 2. This experiment was conducted for the first day of winter and summer for Auckland city. Semi-transparent and opaque Solar Boundary condition type is used to model the thermal situation of windows, and other walls, respectively, and zero heat flux is applied for the building's thermal condition. One-layer Shell conduction is used for all walls with concrete material properties for considering the effect of building wall conductivity and its impact on thermal resistance between indoor and outdoor environments.

Table 2: solar radiation information for the first day of July and January

First day of July

time	Direct radiation (W/m^2)	Diffusion radiation (W/m^2)	Sun direction vector
9:00	808	111	(0.713, -0.08, 0.69)
11:00	866	92	(0.33, -0.26, 0.90)
13:00	874	75	(-0.14, -0.29, 0.94)
15:00	840	104	(-0.57, -0.17, 0.79)
17:00	724	113	(-0.78, 0.08, 50)
First day of January			
9:00	547	44	(0.71, -0.67, 0.18)
11:00	844	65	(0.32, -0.85, 0.39)
13:00	872	66	(-0.14, -0.89, 0.43)
15:00	731	58	(0.58, -0.76, 0.28)

The student geometry is not modeled, and heat generated from each student is neglected, and the CO_2 source term at the inhabitant zone is used for modeling the CO_2 generation from three students.

2.5 Meshing

The computational boundary domain was discretized using unstructured elements. Mesh independency analysis was performed at four different mesh element sizes, and the average temperature related to each one is listed in Table 3. It can be seen that the monitored value became constant by changing the mesh element size from third to fourth mesh case (deviation of less than 1%). Therefore, the mesh by 2460064 element number is selected for future simulations. The temperature plot for these four grids shown in the direction of height is shown in figure 5, and it can be seen, the temperature result of 2460064 and 3440454 is highly close together. Standard wall function is used for near-wall treatment modeling. Maximum and mean y+ of building walls are 61 and 31, respectively, and it can be concluded that the element size near walls is fine enough.

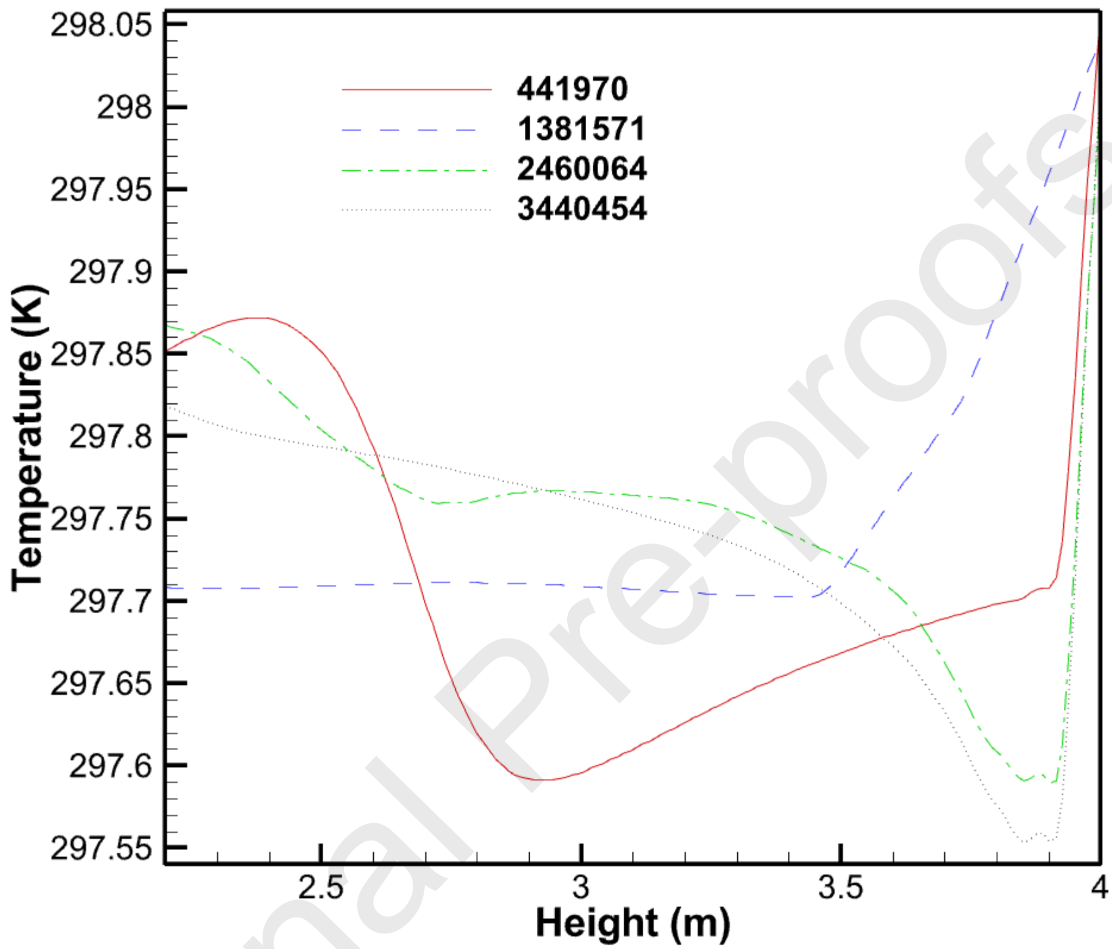

Figure 5. Impact of grid resolution on the temperatures in the direction of height

Table 3: Impact of grid resolution on the selection zone average temperatures.

Mesh name	Number of elements	Average temperature (°C)	Variation (%)
1	441970	24.57	
2	1381571	24.73	0.6
3	2460064	24.58	0.57

4	3440454	24.56	0.09

2.6. Design of Experiment (DOE)

In this study, all factors related to thermal comfort and IAQ are entirely coupled together, and it is not possible to carry out each parameter investigation separately by keeping the constant number for other parameters. Besides, simulation for factorial of all parameter has a high computational cost. Therefore, DOE and Response Surface Methodology were used to decrease the number of experiments and considering whole parameter interaction to evaluating thermal comfort and IAQ. The Central Composite Design (CCD) DOE scheme is used, this model divides each input parameter range into five levels, and the total number of experiments depends on the number of input parameters (K) and F (a phrase invoice to decrease the number of the simulation) based on the formula1, so since the number of input parameters is three and one, respectively, so F is zero, the total number of simulation for summer and winter is fifteen and five respectively. Genetic aggregation is used as a response surface methodology to produce the best response levels based on its CFD simulation output. The advantage of this model has the highest accuracy, reliability, and smoothness. The number of runs for winter and summer for each hour is 5 and 15, respectively. Since four and five different times are simulated for winter and summer, the simulation's total number is 100. A system with 32 cores (2×Xeon 2670) with 32 GB memory was used for this research, while the run time for each simulation was about 6 hours.

Number of design point=$2^{(K-f)}+2k-1$ (8)

Results and Discussion

The chosen latitude and longitude of this city (36.8485°, 174.7633° E) and time zone +12 GMT are applied to represent Auckland's geographical location. The steady-state simulation is performed for five and four different times for summer and winter days, respectively. This procedure applied for two days, the first day of January and July.

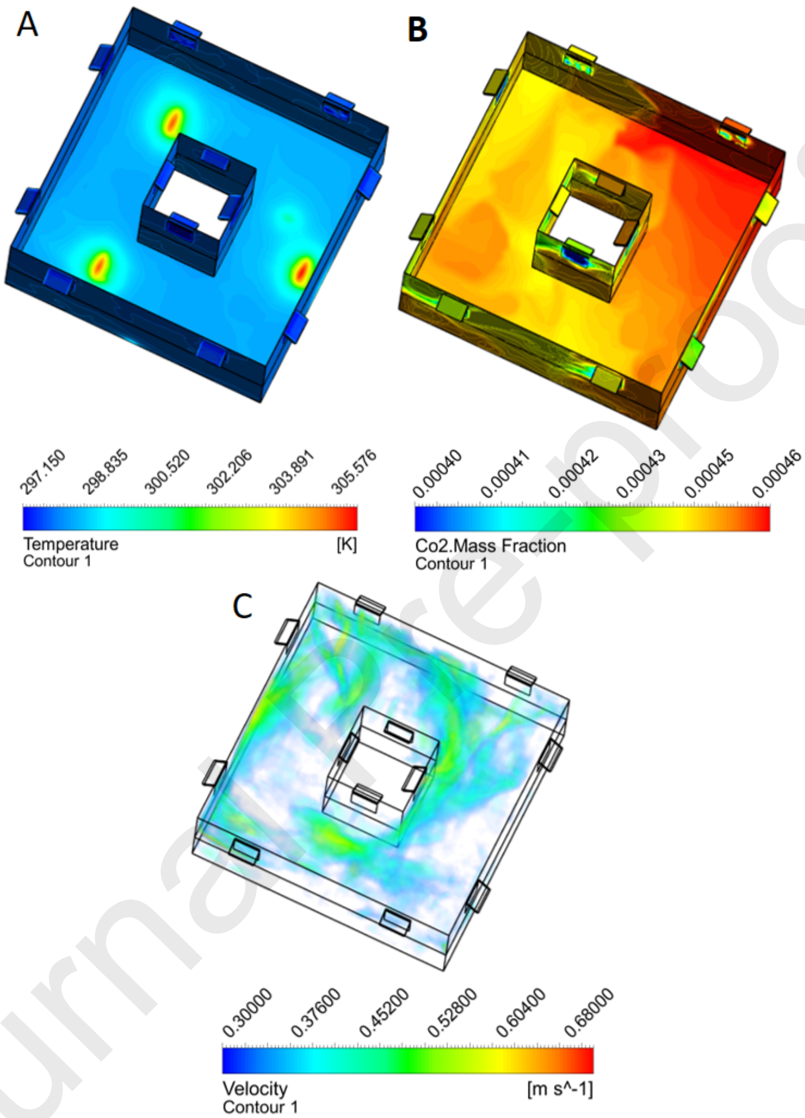

Figure 6. Contours related to 9:00. **A:** Temperature distribution, **B:** CO_2 mass fraction, **C:** 3D buoyancy flow velocity distribution in the hall building.

Figure 6. A and B show the temperature and CO_2 mass fraction distribution on building walls. All parts of Figure 6 are captured from the simulation at 9:00. Hotspot zone caused by direct solar radiation occurs at three different zones at the bottom of the building, and its temperature

magnitude is about 305 K. At the same time, the minimum temperature is 298.5 K, which is one degree higher than the outdoor level. The location, volume size, and peak temperature of these zones will change by various parameters such as time, glazing, and shading conditions. Changing Time leads to a change in temperature distribution within the building. For instance, at 9:00, the solar radiation is on the eastern and southern windows. Here, the hotspot zones can be found close to the eastern side of the building. Another hotspot zone is visible close to the building's western side due to solar radiation passing the southeast windows. The CO_2 mass fraction is higher in the zones far from the windows, resulting in the worst IAQ. There is a strong relationship between temperature, velocity distribution, and CO_2 distribution. Figure 6. C shows the 3D velocity distribution caused by buoyancy flow. The reason for this type of flow in this building is the temperature gradient at various locations. Figure 6 A shows that the temperature distribution is not uniform, and velocity distribution is different based on these temperature gradients. The velocity magnitude inside the hall shows that velocity increases by getting closer to the hotspot zone, and consequently, IAQ is enhanced at these regions, despite the distance from the windows. The minimum and maximum CO_2 mass fraction at this time in the building are 400 and 460 ppm, respectively. The minimum value belongs to the outdoor IAQ situation that causes the locations near to the windows having the CO_2 mass fraction close to this value.

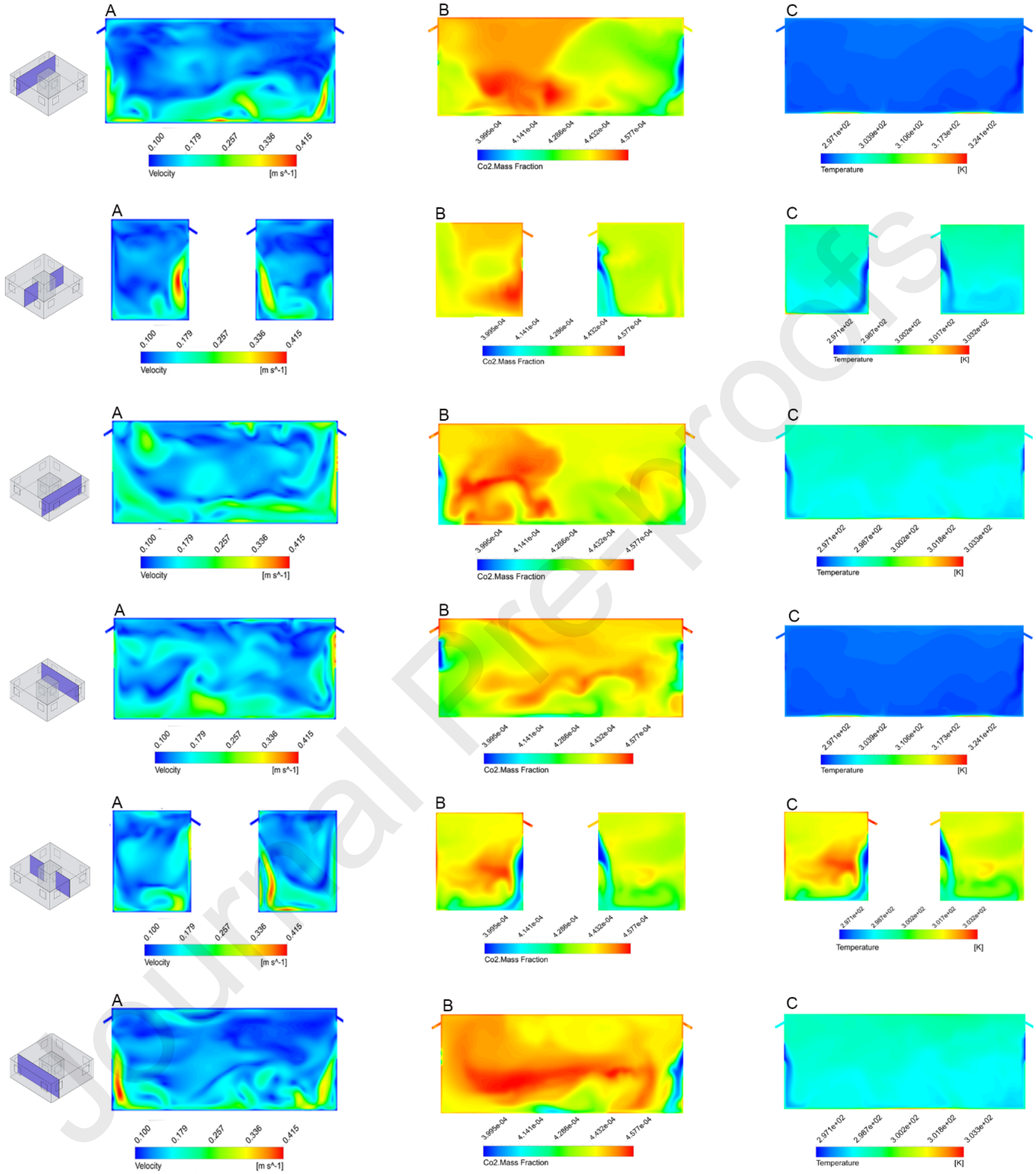

Figure 7. Contours of **A**: Velocity distribution, **B:** CO_2 mass fraction distribution, and **C:** Temperature distribution at various section planes of the summer day.

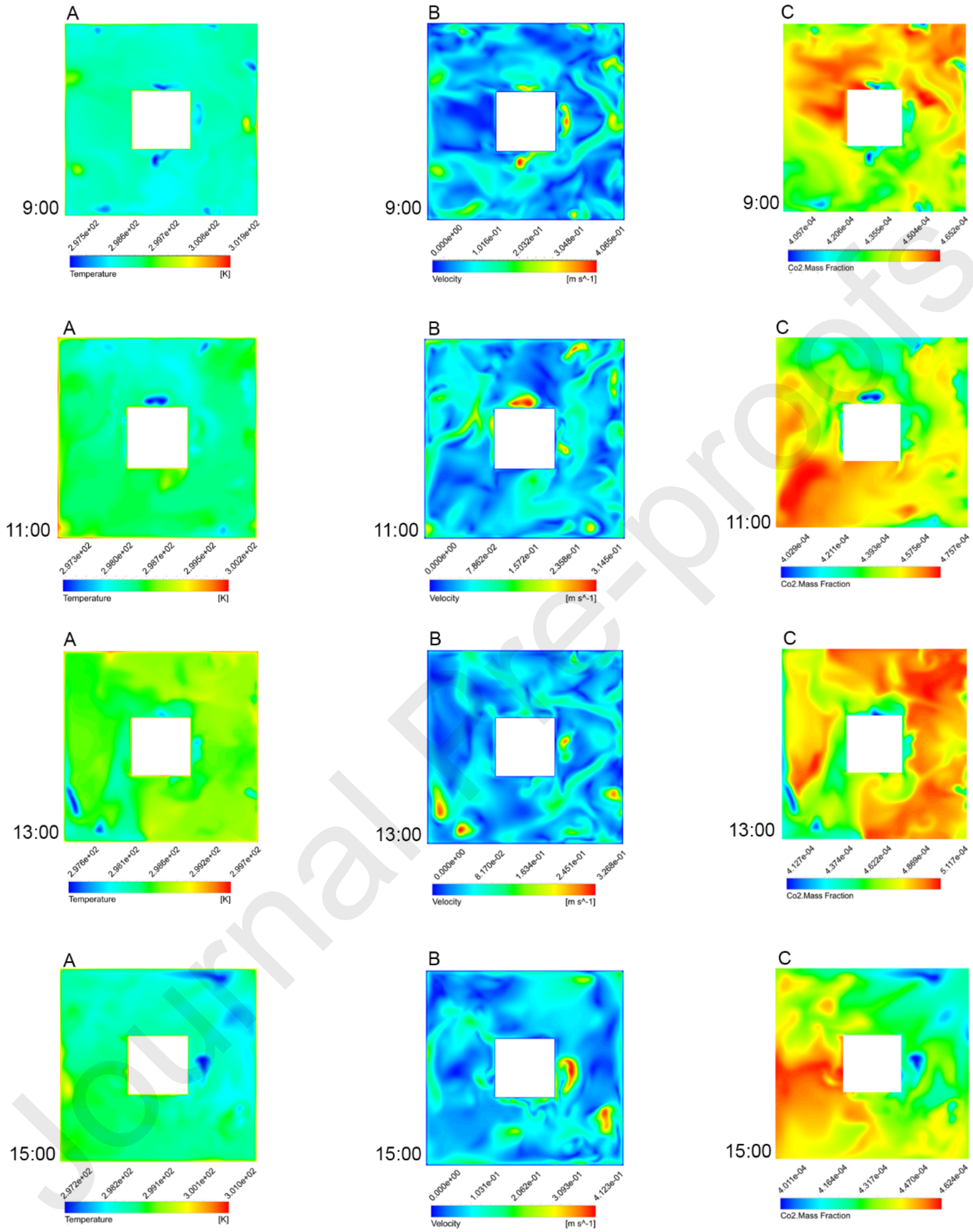

Figure 8. Contours of **A**: temperature distribution, **B**: velocity distribution, and **C**: CO_2 distribution at the level of 0.9m in several hours of the summer day.

Figure 7 A shows the velocity distribution at six different cross-sectional planes. In the absence of outdoor wind speed, maximum velocity is 0.41 m/s. As mentioned, temperature gradients cause velocity distribution as a result of buoyancy. Shading and glazing are the most influencing factors on the temperature distribution. Velocity magnitudes in the zones that are close to windows are higher than other zones. Also, since the maximum temperature gradient is located at the bottom and windows, these zones' velocity is higher than others; therefore, maximum air exchange will occur at these zones. Zones close to the roof stay with the least velocity magnitude and rarely exchange during the time. Figure 7. B and C show the CO_2 mass fraction and temperature distribution at six cross-sectional planes passing through the windows. The zones close to windows have a lower temperature and also a smaller CO_2 mass fraction. All the flow properties such as velocity and temperature and CO_2 mass fraction are entirely coupled together. By comparing the temperature, CO_2 mass fraction, and velocity contours, the hotspot zones and the zones close to windows have higher velocity and lower CO_2 mass fraction.

Figures related to CO2 mass fraction and temperature distribution at middle horizontal and middle vertical planes show the effect of applying windows on the courtyard side. The temperature and CO_2 mass fraction magnitude of zones that are close to courtyard windows are considerably low. So, it can be concluded that using windows on the courtyard is so useful for increasing thermal comfort and IAQ. Figure 8. A shows the temperature distribution at a height of 0.9 m for various times of the day. The maximum temperature at this section at 9:00, 11:00, 13:00, and 15:00 are 302K, 300 K, 299.7, and 301 K, respectively, and there is no high temperature at this height. It is evident that velocity and CO_2 distribution are non-uniform, as shown in Figure 8 B and C, and depend on temperature and velocity, respectively. A higher temperature gradient leads to higher velocity magnitude, and the higher velocity results in a lower CO_2 mass fraction. Furthermore, the

CO_2 mass fraction indirectly depends on the temperature distribution. Velocity distribution depends on the glazing and shading situation, which have been comprehensively analyzed in this research.

3.1 Winter

During the winter, windows are closed; hence, the CO_2 mass fraction inside the room will continuously increase if no active or mechanical ventilation systems are available. Since this study's focus is passive ventilation of buildings, it is evident that by assuming closed windows, improving IAQ is not possible, and therefore the thermal condition is investigated. Using the overhang as a shading tool is neglected because the maximum solar heat gain is desired. The sun's altitude on the winter day is lower than the summer one; therefore, the projected solar radiation magnitude on the inhabitant is higher. Consequently, solar radiation's effect on the selected zone thermal situation is more than summer, despite the outdoor temperature being considerably lower than summer.

Table 4. shows the number of experiments with different windows length is conducted for different hours of the day in winter. This parameter variation on the occupant zone average temperature in the different hours of the day is depicted in Figure 9. This analysis's main target is to find increasing occupant zone temperature due to solar radiation, and It is assumed that all windows are closed and semi-transparent. While the outdoor temperature is 287.15 K and heat transfer interaction with the outdoor environment is possible, there is no flow interaction with the outdoor environment. By increasing the window length (width and length are in equal size), the average total temperature in the occupant zone (the zone with max height 1.8 m) will increase gradually. The variation rate of temperature by increasing windows length is different in different hours, and the magnitude of the average temperature for these hours is approximately the same.

Table 4. different experiments conducted for different hours of the day in winter

Experiment number	Windows length (m)
1	1.12
2	0.75
3	1.5
4	0.93
5	1.31

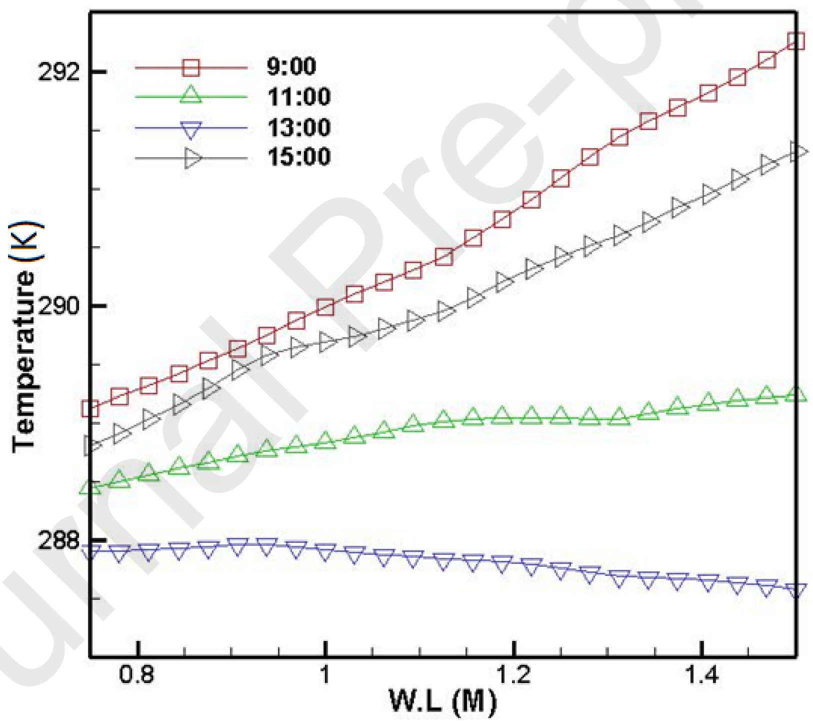

Figure 9. The effect of windows dimension variation on the average temperature of selected geometry

At the lowest windows length (W.L), the average temperature in each hour is close together, but the temperature difference increases by increasing W. L. The average value and variation rate of temperature from the highest to lowest are 9:00, 15:00, 11:00, and 13:00, respectively. W.L variation has no significant effect on the temperature at 13:00 because solar radiation is relatively vertical, and solar absorption from the glazing area is close to zero. Overall, it can be concluded by increasing the W.L, the average temperature will be increased approximately linearly, with a time-dependent rate. This rate is maximum at the first and the last hours of the day. By the way, since these times are the coldest time of a winter's day, a building designer can benefit from this advantage and reduce the considerable energy requirement for heating.

3.2 Summer

Since the temperature range of Auckland city in January is approximately 294.15-297.15 K [62] and is close to the health standard limit, it is assumed that all of the windows are entirely open and have thermal and flow interaction with the outdoor environment. Hence the main parameter that should be investigated is the IAQ, with operating conditions of zero Pascal pressure and 297.15 K temperature. Because there is no mechanical device for ventilation, the main parameter that will affect the IAQ is the temperature distribution that entirely depends on solar radiation magnitude and direction. Solar absorption is influenced by overhang length, overhang angle, and window dimension. For considering all of these parameters on building HVAC situation, DOE is conducted and listed in Table 5. The response surface of temperature and CO_2 mass fraction for each pair of the affective parameter for each hour are extracted and shown in Figure 10 to Figure 14. The input parameters of DOE are overhang length (O.L), overhang angle (O.A), and windows length (W.L) that bound in the range of 0.3 to 0.6 m, 0 to 60 degrees, and 0.75 to 1.5 m, respectively.

Table 5. The experiments that are generated for the summer day

Experiment number	Windows length (m)	overhang length (m)	overhang angle (degree)
1	1.12	0.45	30
2	0.75	0.45	30
3	1.5	0.45	30
4	1.12	0.3	30
5	1.12	0.6	30
6	1.12	0.45	0
7	1.12	0.45	60
8	0.82	0.32	5.60
9	1.42	0.32	5.60
10	0.82	0.57	5.60
11	1.42	0.57	5.60
12	0.82	0.32	54.39
13	1.42	0.32	54.39
14	0.82	0.57	54.39
15	1.42	0.57	54.39

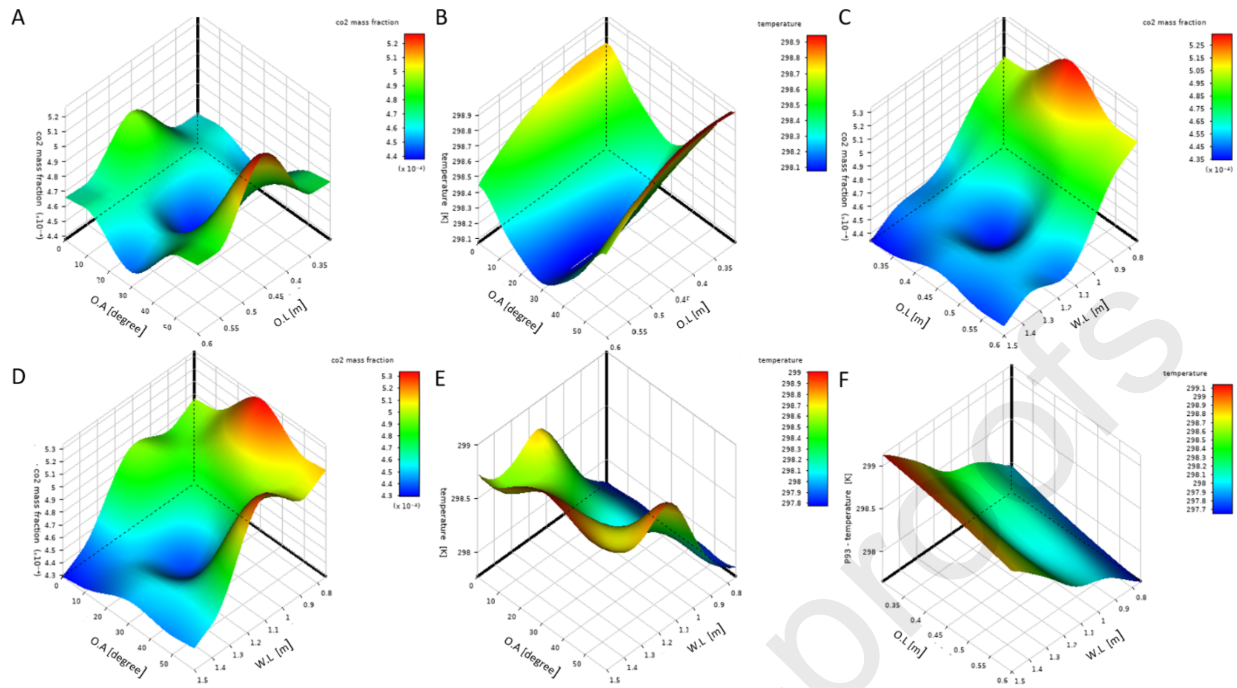

Figure 10. Response Surfaces with Genetic Aggregation at 9:00 **A:** average *CO_2* mass fraction against O.A-O.L, **B:** average temperature against O.A-O.L, **C:** average temperature against O.L-W.L, **D:** average *CO_2* mass fraction against O.A-W.L, **E:** average temperature against O.A-W.L, **F:** average temperature against O.L-W.L.

Figure 10 shows the effect of shading and glazing parameters on the thermal comfort and IAQ at 9:00. The impact of overhang significant parameters on the average CO_2 mass fraction of the occupant zone can be seen in Figure 10 A. At 9:00, solar radiation direction is close to the horizontal, and shading tools are at its lowest performance. CO_2 mass fraction can be reduced up to 80 ppm by controlling the shading tools. Figure 10 B shows the effect of shading tools on the average temperature and reveals that by controlling the shading parameters, the average temperature reduced by 0.8 K. Here, the minimum temperature belongs to the maximum of O.L and in the middle of the O.A range. Increasing O.A leads to reducing the heat fain from the sun, but on the other hand, it decreases the air change with outdoor, and consequently, natural heat transfers with outdoor will be reduced. So, there is an optimum point for O.A . therefore, Figure 10.C illustrates the CO_2 mass fraction by variation of O.L and W.L and is notable that O.L's effect compared to W.L is negligible. Because of increasing air change with increasing windows length, the best IAQ situation occurs at the maximum W.L and causes to reduce the CO_2 mass fraction up to 90 ppm. Figure 10 D presents that the effect of O.A on the IAQ compared to the W.L is negligible. However, by decreasing the O.A, IAQ will be slightly better because increasing overhang angle acts as a barrier in front of the windows, so airflow passing from windows will be decreased, and consequently, the air quality will be worst.

Figure 10 E and 10 F show the effect of O.A-W.L and also O.L-W.L on the average temperature, respectively. It can be seen that the sensitivity of average temperature with windows length variation is higher than effective shading parameters. By increasing the glazing area, due to increasing received solar radiation, the temperature rises dramatically. The response surface of IAQ is opposite of the temperature due to the primary fluid flow caused by the temperature gradient, and since by increasing the area of the window, heat gained will be increased, and the temperature gradient will rise. Therefore, it leads to higher velocity magnitude and more air change per hour (ACH). As a result, the IAQ will be improved significantly.

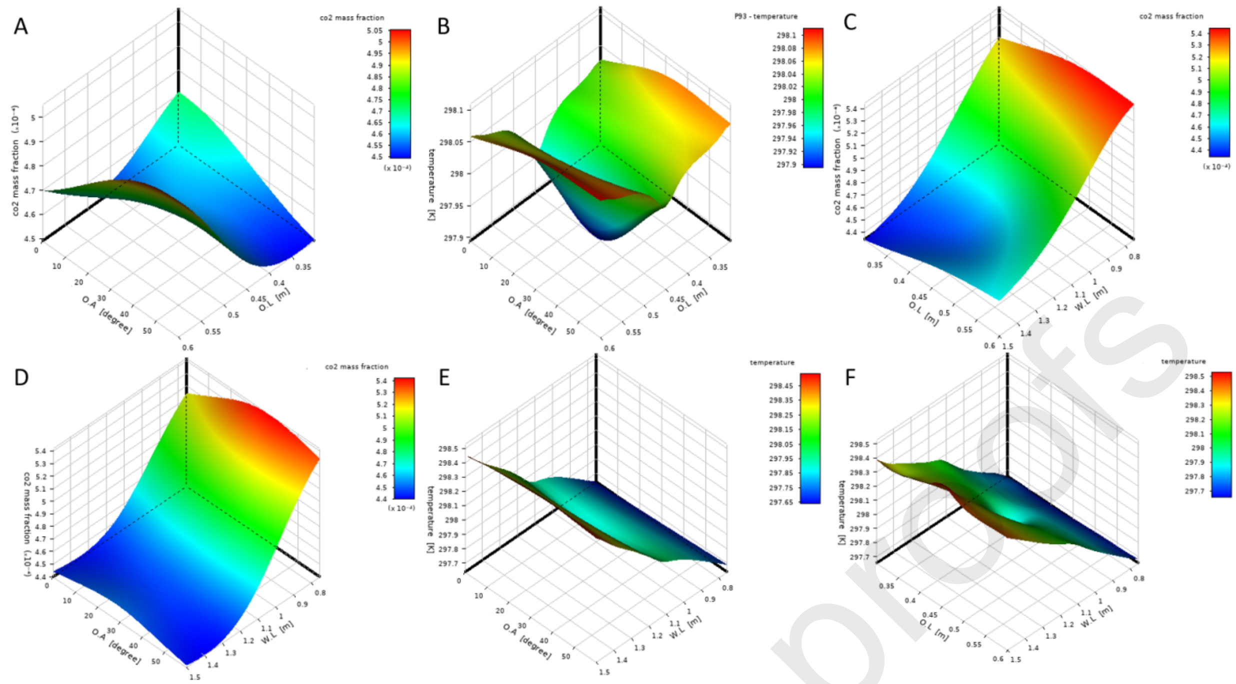

Figure 11. Response Surfaces with Genetic Aggregation at 11:00 **A:** average CO_2 mass fraction against O.A-O.L, **B:** average temperature against O.A-O.L, **C:** average temperature against O.L-W.L, **D:** average CO_2 mass fraction against O.A-W.L, **E:** average temperature against O.A-W.L, **F:** average temperature against O.L-W.L.

Figure 11 A and B show the effect of shading parameters on the CO_2 mass fraction and the average temperature at 11:00. Shading parameters can control the CO_2 mass fraction and temperature up to 50 ppm and 1.1 °C, respectively. Sun altitude at this time is higher than the last time. Therefore, the effect of shading variation parameters on temperature and CO_2 mass fraction is entirely different. It can be seen that the minimum temperature occurs in the middle of O.A and O.L. The peak temperature occurs at maximum and minimum of O.L. Therefore, it can be concluded that the essential factor of shading tools on controlling CO_2 mass fraction is the shading length. CO_2 mass fraction will be reduced by decreasing the O.L and increasing the O.A. from Figure 11 C to F; the impact of shading and glazing parameters interaction on the thermal comfort and IAQ are shown. Due to the higher solar radiation angle, the shading effect on the temperature is higher than 9:00. Nevertheless, it can be seen that the effect of glazing parameter changes on comfort criteria is highly more than shading parameters one.

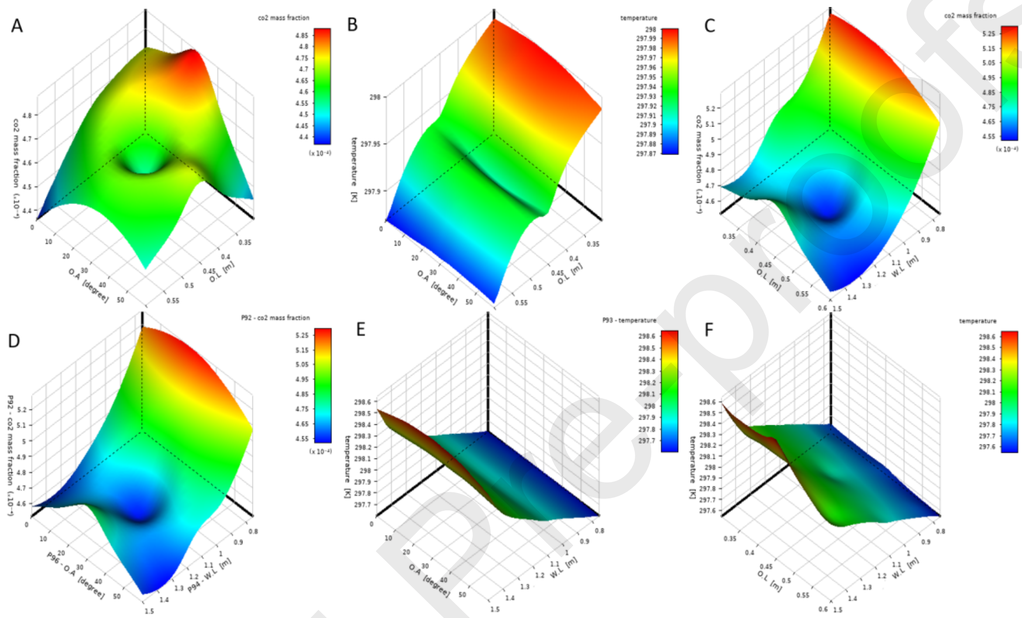

Figure 12. Response Surfaces with Genetic Aggregation at 13:00 **A:** average CO_2 mass fraction against O.A-O.L, **B:** average temperature against O.A-O.L, **C:** average temperature against O.L-W.L, **D:** average CO_2 mass fraction against O.A-W.L, **E:** average temperature against O.A-W.L, **F:** average temperature against O.L-W.L.

Figures 12 A and B illustrate the effect of shading parameter variation on the CO_2 mass fraction and the average temperature on the occupant zone at 13:00. The shading parameter variation has a little lower impact on the average temperature than 11:00, and the maximum difference between the highest and lowest temperature and CO_2 mass fraction is 0.1 K and 40 ppm, respectively. This difference in parameter influence is due to the sun's location, which is approximately perpendicular to the window's perpendicular direction, and shading and glazing parameters are on its minimum effect on the temperature and CO2 mass fraction distribution. Figure 12 C to 12 F shows the response surface of temperature and CO_2 mass fraction by changing the shading and glazing parameters. The sensitivities of IAQ and temperature situation versus shading parameters compared to glazing parameters are negligible. The behavior of CO_2 mass fraction and temperature with W.L's variation is similar to the last time.

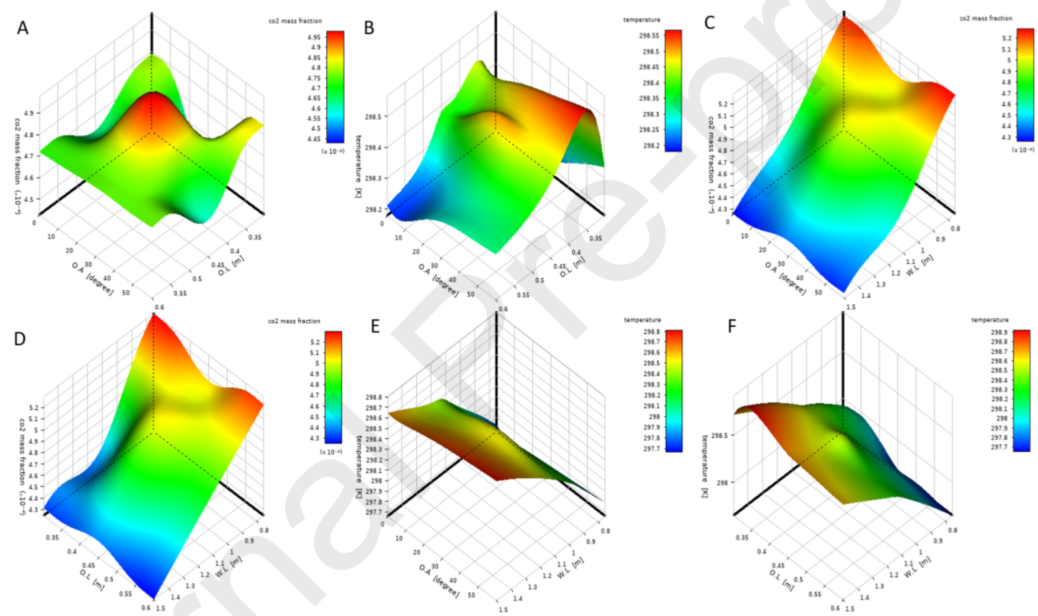

Figure 13. Response Surfaces with Genetic Aggregation at 15:00 **A:** average *CO_2* mass fraction against O.A-O.L, **B:** average temperature against O.A-O.L, **C:** average temperature against O.A-W.L, **D:** average *CO_2* mass fraction against O.L-W.L, **E:** average temperature against O.A-W.L, **F:** average temperature against O.L-W.L.

Figure 13 A and B illustrate the IAQ and thermal situation of the occupant zone at different shading configurations at 15:00. Shading parameters can control the CO_2 mass fraction and temperature in a range of 0.35 K and 50 ppm. The comparison of shading and glazing parameters is similar to previous times in which the shading parameter is less effective on the IAQ and thermal situation (Figure 13 C and 133 F).

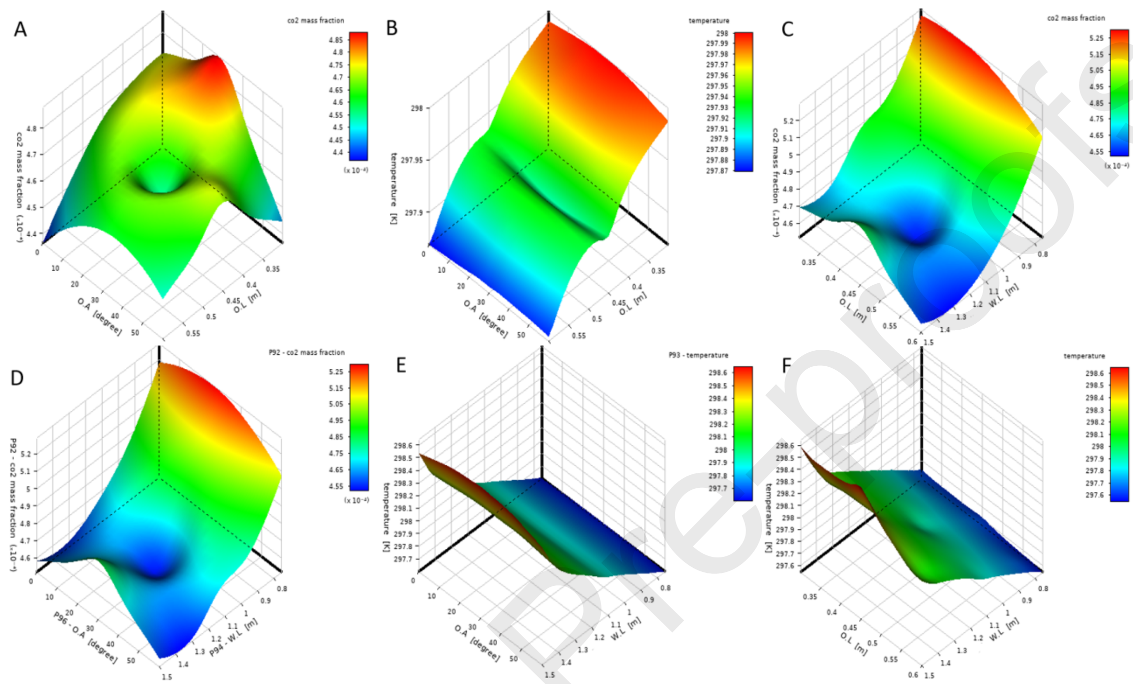

Figure 14. Response Surfaces with Genetic Aggregation at 17:00 **A:** average CO_2 mass fraction against O.A-O.L, **B:** average temperature against O.A-O.L, **C:** average temperature against O.L-W.L, **D:** average CO_2 mass fraction against O.A-W.L, **E:** average temperature against O.A-W.L, **F:** average temperature against O.L-W.L.

Figures 14 A and 14 B illustrate the shading parameter effect on the CO_2 mass fraction and temperature situation at 17:00. The shading parameters can control the IAQ situation up to 45 ppm while the best situation occurs at the maximum O.L, and min O.A. thermal condition does not depend on O.A and O.L at this time very much. These parameters can control the temperature up to 0.1 K. However, by comparing this response surface to the glazing parameter's effect, it can be seen that shading parameter variation has fewer effects on the thermal condition, and the thermal response ratio is about 10% of glazing parameters. The effect of the glazing parameter at this time is like the previous time with a lower rate, while it can be seen that the effect of shading parameters can be neglected.

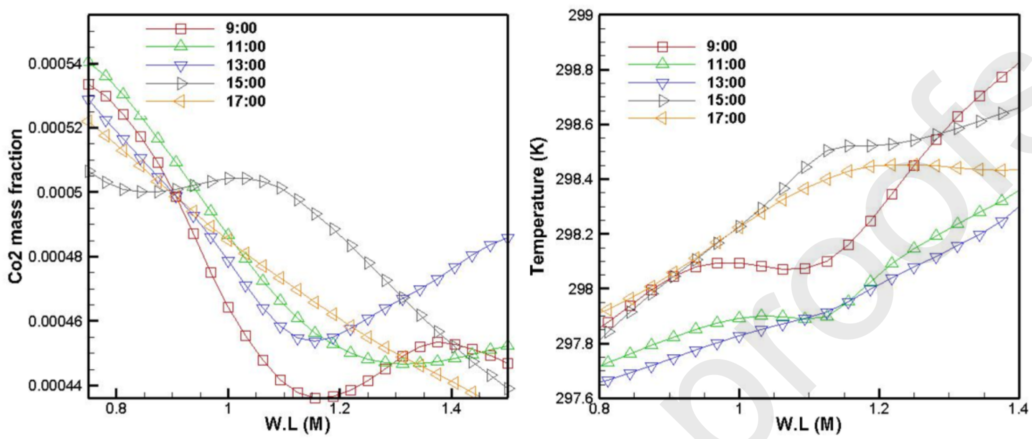

Figure 15. A: Effect of W.L variation on the average CO_2 mass fraction, **B:** Effect of W.L change on the average temperature

Figure 15 A shows the effect of windows length on the CO_2 mass fraction in the occupant zone for several hours. Since interpreting the effect of glazing variation is difficult separately via 3D plots, this figure shows the effect of windows dimension variation on the thermal situation and CO_2 mass fraction of the occupant zone. These results are captured by keeping the shading parameters constant in the middle of its bands. Increasing the W.L to 1.2 for all cases increases the air change per hour (ACH). The trends of CO_2 mass fraction variation are monotonically decreased in all cases. By increasing W.L, this reduction will continue at 15:00 and 17:00, but at other times it starts to rise in a finite band. Overall, by increasing the W.L, the temperature will increase. However, there is a small fluctuation at 9:00 and 17:00, that approximately temperature remains constant in a short-range. This phenomenon occurs since by increasing the glazing area, solar heat gain will increase, and on the other side, ACH will rise, and finally, heat transfer with the outdoor environment enhances.

Consequently, temperature and CO_2 mass fraction fluctuate in a narrow band. One of the most critical results of RSM is the sensitivity analysis of output parameters VS input parameters. In this research, the thermal situation and CO_2 mass fraction VS shading and glazing parameters are studied.

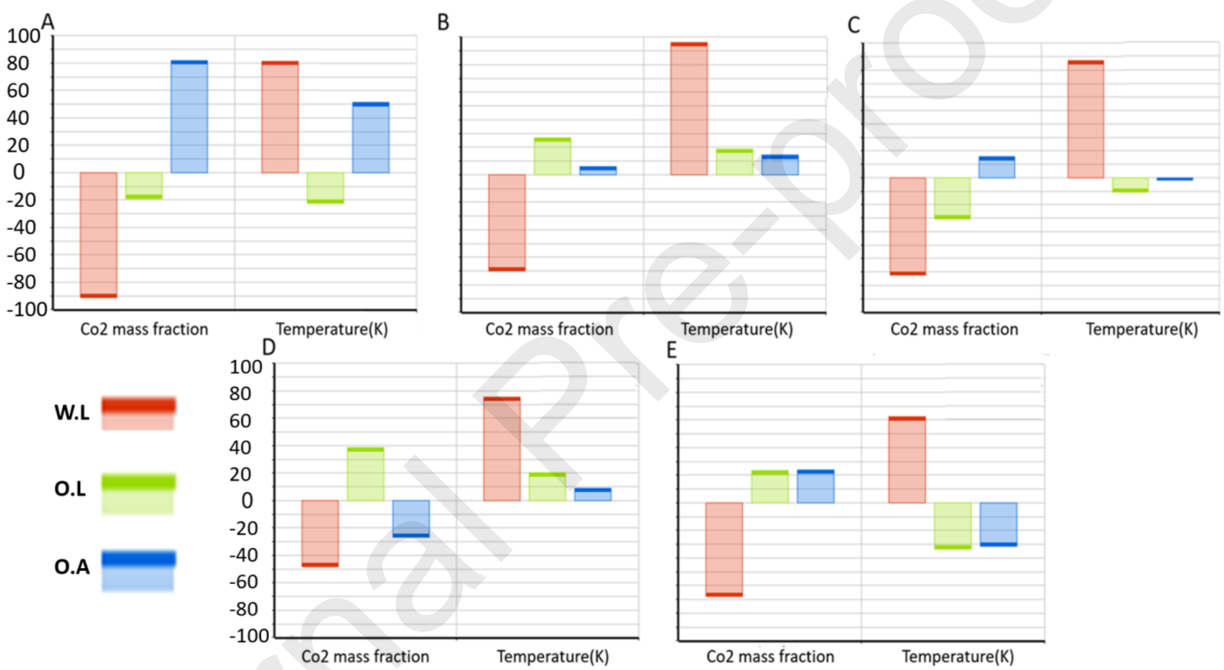

Figure 16. Local sensitivity (percentage) analysis for five different times of a summer day **A:** 9:00, **B:** 11:00, **C:** 13:00, **D:**15:00, **E:** 17:00.

Figure 16 illustrates the local sensitivity analysis of the output parameters for three input parameters at five different times. These sensitivities can be positive or negative and show the direct and inverse relation of these input parameters to output parameters. Input parameters are windows length (W.L), overhang length (O.L), and overhang angle (O.A), and output parameters are average CO_2 mass fraction and temperature of occupant zone. These analyses are extracted in the middle of shading and glazing parameter bands. At all times, the most sensitive parameter is W.L. For instance, at 9:00, it is evident that the window's dimension is the most sensitive factor for changing the situation of thermal comfort and IAQ (80 % and 90%, respectively). The second substantial sensitive factor for both output parameters is O.A. The sensitivity of the CO_2 mass fraction to this parameter is similar to W.L and is 80%. This parameter's temperature sensitivity is 50%, while O.L sensitivity is low compared to other parameters and is about 20% for both output parameters. At 11:00, shading parameters sensitivity for IAQ and thermal situation is very low and is about a third and fifth of W.L sensitivity, respectively.

At 13:00, the thermal situation highly depends on the glazing parameters, and the effect of shading parameters compared to the glazing parameter can be neglected. In contrast, the shading parameter has a substantial impact on the IAQ situation. At 15:00 shading parameter has a significant impact on the IAQ, and its effect is close to W.L ones, and the point is that O.L sensitivity is positive. So, it can be concluded that by increasing O.L, IAQ will be worse, although O.A has a positive sensitivity. At 17:00, both shading parameters have the same sensitivity. Increasing their magnitude is harmful to the IAQ situation and positive for the thermal condition, and the sensitivity of the glazing parameter on the output parameter is higher than two times of shading ones.

The genetic aggregation is applied to reach the high accuracy response surface, and exact input design points for achieving this response variable have been extracted and listed in this Table5. Based on this table, the Input design point can be set via actuators and applied in each hour to reach the best thermal and IAQ situations. The advantage of DOE and RSM in designing smart building HVAC can be seen in this table. The final achievement of using these methods is reaching a smart engine that output variables can be predicted instantly vs. input variables. Input parameters can be controlled via the HVAC actuator, and it means that for reaching a desired thermal and IAQ situations, requirement shading and glazing actuator situation can be predicted without any further CFD simulation.

Table 6. Maximum and minimum CO_2 mass fraction and temperature in several hours

W.L (m)	O.L (m)	O.A (degree)	CO_2 mass fraction	Temperature (K)	
1.5	0.3	0	Min:0.000427	298.87	at 9:00
0.75	0.45	30.81	Max: 0.00427	297.77	
0.75	0.6	1.88	0.000497	Min:297.62	
1.5	0.3	32.13	0.000435	Max:299.13	
1.5	0.3	60	Min:0.00043	298.42	at 11:00
0.75	0.6	56.31	Max:0.000564	297.70	
0.75	0.3	0	0.000524	Min:297.63	
1.5	0.45	34.41	0.000452	Max:298.52	
1.33	0.6	0	Min:0.000428	298.06	at 13:00
0.75	0.34	15.12	Max:0.000532	297.61	
0.75	0.6	0	0.00049	Min:297.53	
1.5	0.44	29.31	0.000486	Max:298.64	
1.5	0.6	0	Min:0.000422	298.54	at 15:00
0.75	0.32	4.62	Max:0.000563	297.97	
0.75	0.6	8.65	0.000528	Min:297.59	
1.5	0.34	60	0.000434	Max:298.98	
1.5	0.3	27.28	Min:0.000426	298.66	at 17:00
0.75	0.59	60	Max:0.000559	297.75	
0.75	0.6	60	0.000559	Min:297.74	
1.5	0.31	4.40	0.000428	Max:297.77	

Moreover, aiming to achieve comfort temperature and desired CO_2 mass fraction, the input parameter that leads to this result should be calculated to be applied to the HVAC actuators.

The maximum CO_2 mass fraction occurs at 17:00, and its magnitude is 559 ppm, which is 159 ppm higher than the outdoor CO_2 ppm. Conditions that lead to this situation are 0.75 m, 0.599 m, and 60 degrees for W.L, O.L, and O.A, respectively. On the other side, minimum CO_2 mass fraction occurs at 15:00 by 422 ppm by applying 1.5 m, 0.6 m, and zero degrees for the W.L and O.L and also O.A. maximum and minimum temperature occurs at 9:00 and 17:00 by 299.13 K and 297.53 K that is 2 K and 0.38 K higher than outdoor temperature respectively. Moreover, the condition to reach these results is 1.5 m, 0.3 m, 32.13 degrees, and 0.75, 0.6, and 0 degrees, respectively.

4. Conclusion

A systematic evaluation of the 3D steady RANS CFD simulations has been conducted to assess the effect of shading and glazing parameters on the thermal situation and indoor air quality variations. For this purpose, the DOE with genetic aggregation RSM is used to reduce the number of experiments and predict those parameter interaction effects.

The main concluding points of this paper are:

- Glazing parameters can control the temperature higher than 3 degrees in winters, while the maximum temperature variation is about 1.6 degrees on the summer day.
- In summer days, the variation rate of temperature and CO2 mass fraction VS. Glazing parameter (W.L) is approximately positive. However, the situation is more complicated in shading parameters.
- The thermal comfort and IAQ sensitivities for Glazing parameters is higher than that of shading ones. This maximum sensitivity of temperature for the glazing parameter is about 95%, occurs at 11:00 while for shading ones is 50%, and occurs at 9:00. The maximum glazing and shading parameter sensitivity to control the CO2 mass fraction is 90% and

80%, respectively, at 9:00. So it can be concluded that the maximum sensitivity of building average temperature and CO2 mass fraction to glazing and shading parameters belongs to the earliest time of the school official day.

- Appropriate shading and glazing configuration for each time is different, and for reaching the best comfort in each hour, dynamic shading and glazing should be designed.
- On the winter day, the temperature variation rate is almost linear regarding the window dimensions, but this function is more complex and nonlinear in the summer.

It can be concluded that glazing tools can compensate for a significant amount of required heating energy in winter. On the other hand, by using shading devices and opening windows, air quality can be controlled significantly in this school. Finally, further research is needed to study ambient wind velocity, building orientation, courtyard shape, and dimensions on the thermal comfort and indoor air quality in schools. Moreover, the different populations of students can be modeled, and the effect of their geometry and heat generation can be considered. Considering the primary purpose of this paper and DOE approaches limitations, the input parameters interaction effect on the output parameter variation is studied. Therefore, another factor that can be considered in future research is applying an active air-conditioning system or modeling a building with highly glazing and opening windows and finding the appropriate configuration systems to reach the desired thermal comfort and IAQ. Hereupon, local comfort investigating (PMV and PPD) can be considered in future works.

References

[1] B. Bajcinovci, F. Jerliu, Achieving energy efficiency in accordance with bioclimatic architecture principles, Environmental and Climate Technologies 18(1) (2016) 54-63.
[2] A. Kamenders, L. Vilcane, Z. Indzere, D. Blumberga, Heat demand and energy resources balance change in Latvia, Energy Procedia 113 (2017) 411-416.
[3] R.K. Nath, M.F.M. Zain, M. Jamil, An environment-friendly solution for indoor air purification by using renewable photocatalysts in concrete: A review, Renewable and Sustainable Energy Reviews 62 (2016) 1184-1194.
[4] A. Challoner, L. Gill, Indoor/outdoor air pollution relationships in ten commercial buildings: PM2. 5 and NO2, Building and Environment 80 (2014) 159-173.
[5] Q. Wang, A. Ploskić, X. Song, S. Holmberg, Ventilation heat recovery jointed low-temperature heating in retrofitting—An investigation of energy conservation, environmental impacts and indoor air quality in Swedish multifamily houses, Energy and Buildings 121 (2016) 250-264.
[6] Z.S. Zomorodian, M. Tahsildoost, M. Hafezi, Thermal comfort in educational buildings: A review article, Renewable and sustainable energy reviews 59 (2016) 895-906.
[7] O. Langniss, K. Seyboth, L. Beurskens, A. Wakker, Renewables for heating and cooling-untapped potential, Policy Studies 2012 (2013) 2011.
[8] L.D. Pereira, D. Raimondo, S.P. Corgnati, M.G. da Silva, Assessment of indoor air quality and thermal comfort in Portuguese secondary classrooms: Methodology and results, Building and Environment 81 (2014) 69-80.
[9] J. Al-Hubail, A.-S. Al-Temeemi, Assessment of school building air quality in a desert climate, Building and Environment 94 (2015) 569-579.
[10] J. Jiang, D. Wang, Y. Liu, Y. Xu, J. Liu, A study on pupils' learning performance and thermal comfort of primary schools in China, Building and Environment 134 (2018) 102-113.
[11] P. Wargocki, J.A. Porras-Salazar, S. Contreras-Espinoza, The relationship between classroom temperature and children's performance in school, Building and Environment 157 (2019) 197-204.
[12] E. Finell, U. Haverinen-Shaughnessy, A. Tolvanen, S. Laaksonen, S. Karvonen, R. Sund, V. Saaristo, P. Luopa, T. Ståhl, T. Putus, The associations of indoor environment and psychosocial factors on the subjective evaluation of indoor air quality among lower secondary school students: a multilevel analysis, Indoor air 27(2) (2017) 329-337.
[13] C. Vornanen-Winqvist, S. Toomla, K. Ahmed, J. Kurnitski, R. Mikkola, H. Salonen, The effect of positive pressure on indoor air quality in a deeply renovated school building–a case study, Energy Procedia 132 (2017) 165-170.
[14] L. Asere, T. Mols, A. Blumberga, Assessment of energy efficiency measures on indoor air quality and microclimate in buildings of Liepaja municipality, Energy Procedia 95 (2016) 37-42.
[15] ASHRAE, Ventilation for acceptable indoor air quality, 2019.
[16] R.J. De Dear, G.S. Brager, Thermal comfort in naturally ventilated buildings: revisions to ASHRAE Standard 55, Energy and buildings 34(6) (2002) 549-561.
[17] B.W. Olesen, K. Parsons, Introduction to thermal comfort standards and to the proposed new version of EN ISO 7730, Energy and buildings 34(6) (2002) 537-548.
[18] M. Griffiths, M. Eftekhari, Control of CO2 in a naturally ventilated classroom, Energy and Buildings 40(4) (2008) 556-560.
[19] D.Q.L.S. Branz, Ventilation & Indoor Air Quality, Ministry of Education (2007).
[20] S. Vilčeková, P. Kapalo, Ľ. Mečiarová, E.K. Burdová, V. Imreczeová, Investigation of indoor environment quality in classroom-case study, Procedia engineering 190 (2017) 496-503.
[21] L. Stabile, M. Dell'Isola, A. Russi, A. Massimo, G. Buonanno, The effect of natural ventilation strategy on indoor air quality in schools, Science of The Total Environment 595 (2017) 894-902.

[22] N.Y.Y. Razali, M.T. Latif, D. Dominick, N. Mohamad, F.R. Sulaiman, T. Srithawirat, Concentration of particulate matter, CO and CO2 in selected schools in Malaysia, Building and environment 87 (2015) 108-116.
[23] G. Guyot, M.H. Sherman, I.S. Walker, Smart ventilation energy and indoor air quality performance in residential buildings: A review, Energy and Buildings 165 (2018) 416-430.
[24] H. Simmler, B. Binder, Experimental and numerical determination of the total solar energy transmittance of glazing with venetian blind shading, Building and Environment 43(2) (2008) 197-204.
[25] A. Kirimtat, B.K. Koyunbaba, I. Chatzikonstantinou, S. Sariyildiz, Review of simulation modeling for shading devices in buildings, Renewable and Sustainable Energy Reviews 53 (2016) 23-49.
[26] W. Platzer, Evaluation of overheating protection with sun-shading, Sol. Energy 69 (2001) 59-74.
[27] H.S. Lim, G. Kim, Predicted performance of shading devices for healthy visual environment, Indoor and Built Environment 19(4) (2010) 486-496.
[28] J. Park, J.-I. Choi, G. Rhee, Enhanced single-sided ventilation with overhang in buildings, Energies 9(3) (2016) 122.
[29] J. Yao, An investigation into the impact of movable solar shades on energy, indoor thermal and visual comfort improvements, Building and Environment 71 (2014) 24-32.
[30] U. Berardi, H.K. Anaraki, The benefits of light shelves over the daylight illuminance in office buildings in Toronto, Indoor and Built Environment 27(2) (2018) 244-262.
[31] F. Soflaei, M. Shokouhian, A. Tabadkani, H. Moslehi, U. Berardi, A simulation-based model for courtyard housing design based on adaptive thermal comfort, Journal of Building Engineering (2020) 101335.
[32] Q. Chen, Ventilation performance prediction for buildings: A method overview and recent applications, Building and environment 44(4) (2009) 848-858.
[33] A. Abdeen, A.A. Serageldin, M.G. Ibrahim, A. El-Zafarany, S. Ookawara, R. Murata, Solar chimney optimization for enhancing thermal comfort in Egypt: An experimental and numerical study, Solar Energy 180 (2019) 524-536.
[34] J.F. De Lisle, The climate of the Auckland Islands, Campbell Island and Macquarie Island, Proceedings (New Zealand Ecological Society), JSTOR, 1965, pp. 37-44.
[35] M. Patricia Denne, A comparison between fruits of Cox's orange pippin from Kent, England, and Auckland, New Zealand, New Zealand Journal of Botany 1(3) (1963) 295-300.
[36] Z. Ge, G. Xu, H. Poh, C. Ooi, X. Xing, CFD simulations of thermal comfort for naturally ventilated school buildings, IOP Conference Series: Earth and Environmental Science, IOP Publishing, 2019, p. 012073.
[37] K. Kosutova, T. van Hooff, C. Vanderwel, B. Blocken, J. Hensen, Cross-ventilation in a generic isolated building equipped with louvers: Wind-tunnel experiments and CFD simulations, Building and Environment 154 (2019) 263-280.
[38] S. Liu, W. Pan, Q. Cao, Z. Long, Y. Jiang, Q. Chen, CFD simulations of natural cross ventilation through an apartment with modified hourly wind information from a meteorological station, Energy and Buildings 195 (2019) 16-25.
[39] G. Elshafei, A. Negm, M. Bady, M. Suzuki, M.G. Ibrahim, Numerical and experimental investigations of the impacts of window parameters on indoor natural ventilation in a residential building, Energy and Buildings 141 (2017) 321-332.
[40] J. Castillo, G. Huelsz, A methodology to evaluate the indoor natural ventilation in hot climates: Heat Balance Index, Building and Environment 114 (2017) 366-373.
[41] V. Costanzo, M. Donn, Thermal and visual comfort assessment of natural ventilated office buildings in Europe and North America, Energy and Buildings 140 (2017) 210-223.

[42] S. Benni, P. Tassinari, F. Bonora, A. Barbaresi, D. Torreggiani, Efficacy of greenhouse natural ventilation: Environmental monitoring and CFD simulations of a study case, Energy and Buildings 125 (2016) 276-286.
[43] J.M. Gimenez, F. Bre, N.M. Nigro, V. Fachinotti, Computational modeling of natural ventilation in low-rise non-rectangular floor-plan buildings, Building Simulation, Springer, 2018, pp. 1255-1271.
[44] H. Montazeri, F. Montazeri, CFD simulation of cross-ventilation in buildings using rooftop wind-catchers: Impact of outlet openings, Renewable Energy 118 (2018) 502-520.
[45] C. Porras-Amores, F.R. Mazarrón, I. Cañas, P.V. Sáez, Natural ventilation analysis in an underground construction: CFD simulation and experimental validation, Tunnelling and Underground Space Technology 90 (2019) 162-173.
[46] J. Park, G.H. Rhee, Comparison of volume flow rate and volume-averaged local mean age of air for evaluating ventilation performance in natural ventilation, Journal of Mechanical Science and Technology 31(12) (2017) 5801-5812.
[47] F. Muhsin, W.F.M. Yusoff, M.F. Mohamed, A.R. Sapian, CFD modeling of natural ventilation in a void connected to the living units of multi-storey housing for thermal comfort, Energy and Buildings 144 (2017) 1-16.
[48] J.A. Castillo, G. Huelsz, T. van Hooff, B. Blocken, Natural ventilation of an isolated generic building with a windward window and different windexchangers: CFD validation, sensitivity study and performance analysis, Building Simulation, Springer, 2019, pp. 475-488.
[49] S. Omrani, V. Garcia-Hansen, B.R. Capra, R. Drogemuller, On the effect of provision of balconies on natural ventilation and thermal comfort in high-rise residential buildings, Building and Environment 123 (2017) 504-516.
[50] Z. Tong, Y. Chen, A. Malkawi, G. Adamkiewicz, J.D. Spengler, Quantifying the impact of traffic-related air pollution on the indoor air quality of a naturally ventilated building, Environment international 89 (2016) 138-146.
[51] S. Gilani, H. Montazeri, B. Blocken, CFD simulation of stratified indoor environment in displacement ventilation: Validation and sensitivity analysis, Building and Environment 95 (2016) 299-313.
[52] Z. Shi, Z. Lu, Q. Chen, Indoor airflow and contaminant transport in a room with coupled displacement ventilation and passive-chilled-beam systems, Building and Environment 161 (2019) 106244.
[53] Z. Chen, J. Xin, P. Liu, Air quality and thermal comfort analysis of kitchen environment with CFD simulation and experimental calibration, Building and Environment 172 (2020) 106691.
[54] D.Y. Park, S. Chang, Effects of combined central air conditioning diffusers and window-integrated ventilation system on indoor air quality and thermal comfort in an office, Sustainable Cities and Society (2020) 102292.
[55] J. Zheng, Q. Tao, L. Li, Wind Pressure Coefficient on a Multi-Storey Building with External Shading Louvers, Applied Sciences 10(3) (2020) 1128.
[56] O. Rouaud, M. Havet, Computation of the airflow in a pilot scale clean room using K-ε turbulence models, International Journal of Refrigeration 25(3) (2002) 351-361.
[57] Q. Chen, Comparison of different k-ε models for indoor air flow computations, Numerical Heat Transfer, Part B Fundamentals 28(3) (1995) 353-369.
[58] J. Bennett, P. Davy, B. Trompetter, Y. Wang, N. Pierse, M. Boulic, R. Phipps, P. Howden-Chapman, Sources of indoor air pollution at a New Zealand urban primary school; a case study, Atmospheric Pollution Research 10(2) (2019) 435-444.
[59] I. Fluent, FLUENT 6.3 user's guide, Fluent documentation (2006).
[60] J.A. Duffie, W.A. Beckman, Solar engineering of thermal processes, John Wiley & Sons2013.

[61] M.L. Pereira, G. Graudenz, A. Tribess, L. Morawska, Determination of particle concentration in the breathing zone for four different types of office ventilation systems, Building and Environment 44(5) (2009) 904-911.
[62] D.B. Frost, A. Auliciems, C. de Freitas, Myocardial infarct death and temperature in Auckland, New Zealand, International journal of biometeorology 36(1) (1992) 14-17.

- evaluate the effect of shading and glazing parameters using genetic aggregation response surface methodology
- ventilation and comfort assessment in a multipurpose hall in Auckland, New Zealand
- Investigation of thermal comfort and IAQ situation using CFD simulation
- Unlike the winter days, building temperature variation respect to windows dimension is nonlinear in the summer days.
- The thermal comfort and IAQ sensitivities for Glazing parameters is much higher than that of shading parameters

Reza Amini: Conceptualization, Methodology, Software, Validation, Data Curation, Visualization, Writing - Original Draft

Amirhosein Ghaffarianhoseini: Supervision, Conceptualization, Methodology, Software, Formal analysis, Visualization, Writing - Original Draft

Ali Ghaffarianhoseini : Visualization, Writing- Review & Editing
Umberto Berard: Visualization, Writing- Review & Editing